Huai, C., Xie, J., Liu, F., Du, J., Chow, D.H.C., Liu, J. Experimental and Numerical Analysis of Fire Risk in Historic Chinese Temples: a Case in Beijing. Journal of Architectural Heritage. (in press)

Experimental and Numerical Analysis of Fire Risk in Historic Chinese Temples: a Case in Beijing

Chaoping Huai[1], Jingchao Xie[1*], Fang Liu[2*], Jiangtao Du[3], David H.C. Chow[3], Jiaping Liu[1]

1. College of Architecture and Civil Engineering, Beijing University of Technology, China;

2. School of Environmental and Energy Engineering, Beijing University of Civil Engineering and Architecture, China;

3. School of Architecture, University of Liverpool, Liverpool, L69 7ZN, UK.

*** Correspondence**:

Jingchao Xie, College of Architecture and Civil Engineering, Beijing University of Technology, No. 100 Pingleyuan, Chaoyang District, Beijing 100124, China; Email: xiejc@bjut.edu.cn

Fang Liu, School of Environmental and Energy Engineering, Beijing University of Civil Engineering and Architecture, No. 1 Exhibition Hall Road, Xicheng District, Beijing 100044, China; Email: liufang@bucea.edu.cn

Abstract

To analyze the extent of fire risk in historic Chinese wooden structure buildings, the fire load characteristics of a historic temple in Beijing were studied. In this paper, the thermogravimetric experiments and cone calorimeter experiments were conducted on raw wood collected from historic Chinese buildings. Based on the experiment results, temple fire experiments were conducted in a full-scale model temple with high fire load in a historic Chinese wooden structure temple. FDS software was used to explore the characteristics of fire growth and spread in the initial fire. The results demonstrated that the pyrolysis kinetics parameters of historical wood were smaller than those of fresh wood. The reference temperature at 150℃ with wood density of 410 kg/m^3 in wooden structure building fire simulation was relatively credible. It's easier to occur flashover in historic wooden structure buildings of a lower wood density and pyrolysis parameters.

Keywords: Wooden structure, Fire risk, Pyrolysis parameters, FDS, Historic Chinese Temple, Fire spread

1. Introduction

Heritage building is a listed building of historical and cultural significance, which show the accomplishments of past eras and is non-renewable. (Bernardini et al. 2016; Zhou et al. 2018; Chorlton and Gales 2019, 2020). In Beijing, a large proportion of accredited historical buildings are wooden structures, which is a special kind of frame structure with unique dou gong (corbel brackets) and tenon joints used as connections, especially the roof structures with large exposed timber surfaces. (Durak, Erbil and Akıncıtürk 2011; Regueira and Guaita 2018). Ibrahim et al. (2011), Li, Yu, and Yu (2012) and Schmid et al. (2014) concluded that the fire resistance rating of historic architecture is low, its flammable objects with good combustion conditions, which belongs to level 3 to level 4 fire resistance. Many attempts have proposed to develop approaches that address the fire risks of historic buildings (Watts and Solomon 2002; Zhou, Zhou, and Chao 2012). Meanwhile, Lowden and Hull (2013) and Altun, Doğan, and Bayraml (2016) studied the flammability behavior of wood and methods for its reduction. Chen etc. (2018) discovered that radiation heat contributed significantly towards promoting fire spread on a sloped roof. Emberley et al. (2017) and Bartlett et al. (2017) carried out compartment fire tests with multiple exposed timber surfaces. The test results are helpful to the analysis of fire development process in wooden buildings.

The State Administration of Cultural Heritage and the Ministry of Public Security issued the Ten Provisions on Fire Safety Management of Cultural Relics (Ten Provisions on Fire Safety Management of Cultural Relics. 2015). Matsushima and Takaya (2017) and Neto and Ferreira (2020) studied that although the fire safety regulations for historic timber buildings have been documented and a large number of suggestions have been offered to reduce fire risks of these

buildings, fires still broke out frequently in historic buildings recently.

Due to the complex wooden structures, high fire load density, aging electrical lines and lack of targeted fire protection measures, most historic buildings are faced with serious fire threats as they can be damaged by flame, heat, smoke, falling debris, together with inappropriate fire measures (Chow and Chow 2010; Huang et al. 2011; Zheng and Liu 2013; Dong, You, and Hu 2014; Tung et al. 2018). Moreover, wood materials decay over time owing to the presence of aggressive environmental conditions, which is easy to be ignited and spread rapidly with a lower wood density (Östman and Tsantaridis. 2016; Meng et al. 2018). Pyrolysis is a key process in all stages of wood burning from ignition to extinction (Richter and Rein 2020). Besides, the pyrolysis temperature and reaction heat of timber are two important parameters for fire analysis of timber buildings (Poletto et al. 2012; Gašparovič et al. 2012; Tapasvi et al. 2013; Tian et al. 2016). Only by inputting scientific and reasonable pyrolysis parameters can the fire dynamics process be simulated more accurately.

Fire Dynamics Simulator (FDS) is widely used among fire study groups to simulate building fires, including smoke and flow characteristics (Chen et al. 2010; Byström et al.2012; Weinschenk, Overholt, and Madrzykowski 2016; Tung et al. 2018). In literature, most fire models of wooden building are relatively simple and the models maybe not advanced enough, resulting in less accuracy for fire simulation in compartments with combustible structural materials (Östman, Brandon, and Frantzich 2017). Besides, few large-scale fire experiments have been carried out on historic wooden buildings, therefore, additional full-scale tests with pyrolysis parameters of historical wood are needed to provide information on fire spread.

The objective of the present study was to provide insights into fire growth and spread in historic

wooden structure buildings as limited information was available for this fire scenario. To analyzed the fire risk of an accredited historical temple in use in Beijing, in situ fire load surveys was conducted. Besides, wood thermogravimetric experiments and cone calorimeter and electronic balance tests were carried out to obtain pyrolysis kinetics parameters and physical parameters of historical wood samples. Thus, room fire experiments with scientific and reliable parameters were conducted in a full-scale model temple equipped with both movable and fixed fire loads. Numerical simulations were then carried out by FDS software to predict the fire growth and spread characteristics. Furthermore, comparative experiments were conducted to demonstrated the input parameter settings affecting the fire spread. Finally, some feasible protection measures were put forward.

2. Methodology

2.1 Temple building studied

2.1.1 Architectural features, structure and furniture

The temple is over 600 years, which is a royal temple constructed with wood and brick, the dimensions of the temple are 21 m by 51 m and 19 m in height, as shown in Figure 1. Walls with a thickness of 0.9 m consisted of wooden framing and stone. Fourteen fixed wooden-structure windows & doors faced south, with the total areas of 280 m^2. The interior timber structure is complicated with beams, columns and eave rafters, which are joined together in a close-knit structure. There are many wooden exhibits on display in the temple. Large areas of timber structures and wood exhibits make it at a great fire risk. This type of structure is one of the most representative in historical buildings with different amounts of fire loads were arranged on both sides of the temple. Besides, detailed architectural drawings of this historical

temple were also provided.

The temple was divided into three areas (A1, A2, A3) to show the wood furniture positions and dimensions from the temple, as shown in Figure 2 & 3, including displaying desks, wooden shelf, wooden sculpture and wooden building model.

Figure 2 shows the furniture from the temple (used for fire safety simulations).

Figure 3 shows the positions and dimensions of the furniture.

2.1.2 Fire loads of temple structure and materials

The total floor area investigated amounted to 982.36 m^2. The fixed and movable fire loads survey results were shown in Table 1 and 2. The total fixed fire load was about 4,107,377 MJ, including wooden pillars, purlines, mortice joints, beams, rafters, roof board and wooden wall (incl. windows & doors) and the fire load belong to roof accounted for about 71.9%. Besides, the fixed fire load density (average heat of combustion) was about 4383.88 MJ/m^2. The movable fire load was about 953,099 MJ, including display desks, wooden shelf, wooden sculpture and wooden building model and the movable fire load density was about 970.21 MJ/m^2. The total value of fixed and movable fire load density was 5354.09 MJ/m^2.

The fire load density of modern residential buildings in house and office is 780 MJ/m^2 and 420 MJ/m^2 separately (Zhu et al. 2008). Compared to the fire load density of the historical temple (5354.09 MJ/m^2), which is about 6.86 times and 12.75 times that of the house and the office.

2.2 Experiment: wood thermogravimetric experiment and cone calorimeter test

The wood thermogravimetric experiments were carried out by German NETZSCH Thermal Analyser (Wen et al. 2004) in the Key Laboratory for Thermal Science and Power Engineering of Ministry of Education, in Tsinghua University, Beijing. The wood samples were collected

from the historic wooden temple in Beijing, which were part of remnants of wood repairs from Beijing Municipal Administration of Cultural Heritage, shown in Figure 4.

- For testing: the wood powder was produced according to the GB 2677 (2004). 1-8 standard method.
- The experimental conditions: (1) Atmosphere: air; (2) Gas flow rate 50 ml/min; (3) Heating rate 5 K/min; (4) Sample amount 5 mg.

The pyrolysis behaviour of the wood samples is determined by thermogravimetry (TG) and derivative thermogravimetry (DTG) (Cordero 1989). The results of thermogravimetry were showed in Figure 5. TG curve showed the change of sample mass with temperature, DTG curve showed the rate of mass variation, and the peak point of DTG indicates the maximum mass loss rate (Mohomane, Motaung, and Revaprasadu 2017; Wang, Jia, and Xin 2017).

According to a previous work, Pre-exponential factor and apparent activation energy were obtained based on the kinetics equations of wood pyrolysis reaction and the thermogravimetric analysis (TGA) data (Bianchi et al. 2011; Sanchez-Silva et al. 2012; Matheus, Zattera, and Santana 2012), the results were shown in Table 3. The minimum of the pyrolysis kinetics parameters was White pine, with a Pre-reference factor of 3.08×10^5 1/min and an apparent activation energy of 75,120 kJ/kmol. The pyrolysis kinetics parameters of Red pine and Nanmu were higher than those of Spruce. The maximum of the pyrolysis kinetics parameters was Fir, with a Pre-reference factor of 2.12×10^6 1/min and an apparent activation energy of 83,020 kJ/kmol.

Table 4 presents the physical parameters of wood samples by cone calorimeter and electronic balance tests. It can be seen that the water content of the four kinds of historical wood has little

difference, ranging from 4.65%~5.79%. The average calorific value of the original wood samples was 23.9 MJ/kg of White pine, 19.2 MJ/kg of Red pine, 18.6 MJ/kg of Spruce and 13.6 MJ/kg of Nanmu. In addition, density of Nanmu and White pine was 561.8 kg/m^3 and 505.9 kg/m^3 separately, which was much higher than that of other two. Density of Red pine (413.7 kg/m^3) and Spruce (386.0 kg/m^3) was similar, while density of Spruce was the lowest.

2.3 Numerical simulation settings

2.3.1 Brief introduction of FDS

This paper used Fire Dynamics Simulation (FDS) version 5.0 2012 to simulate the fire in the temple. FDS is a fire dynamics simulation tool, developed by the National Institute of Standards and Technology. Based on the theories of combustion, fluid mechanics, and thermodynamics, FDS can accurately simulate different fire scenarios, which is widely used in fire science engineering (McGrattan et al. 2007; Hadjisophocleous and Jia 2009; Sun et al. 2011).

2.3.2 Settings of simulations using FDS

The temple model was built by Pyrosim, which is a pre-processing software developed for FDS. The plausible model consists of fixed and active fire loads. The size of fixed fire loads was based on the architectural drawings, the size of active fire loads was measured through field investigation. The wooden pillars, purlines, mortice joints, beams, rafters, roof board and wooden wall (incl. windows & doors) were the components of the fixed fire loads, whereas the active fire loads are the furniture and booth, including displaying desks, wooden shelf, wooden sculpture and a wooden building model, as illustrated in Figure 3. The fire loads were all defined as the same kind wood, for example, Spruce. To ensure the accuracy of calculation, a

grid-independent tests were performed in the simulation workstation. We finally set a mesh of 0.27 m × 0.27 m × 0.27 m with a total number of 1.5552 million grids. The boundary conditions were set in consistent with the external environment, and the ambient temperature was 20°C. Windows & doors were kept open throughout the experiment on the southern side of the temple. Based on the investigation of the fire load calculation, the temple was in accordance with the rapidly fire type, with a fire growth index of 0.0469 kW/s^2, and choosing t^2 type as the fire source type. The fire position was set under the showcase, the power of per unit fire source area was 240 kW (Lu, W.-L. and J.-X. Cheng, 2012). In order to explore the fire spread characteristics before the flashover (the early stage of fire spread) in the historical building, the simulation was terminated at 800 sec. Simulation data for the FDS model, including temperature, heat-release rates, smoke concentration, the visibility variation and CO_2 & CO concentration were obtained from FDS files. Seven thermocouples were located at different heights above the fire source. Two temperature slices were set at the center of the fire source to reflect the temperature variation during the fire spread.

2.3.3 The judgement of flashover

The critical conditions of the occurrence of a flashover are of great significance to the prevention and control of fires. Hao and Hadjisophocleous (2011) and Chow and Chow (2010) discussed that flashover is the most important phenomenon involved in fire, which marks the transition from the early stage of the fire (pre-flashover) to the fully developed fire. Flashover is the term describing a sudden increase of temperature with the fire jumping from the growth stage to the development stage, which marks the beginning of the full development phase of fire, after which the indoor temperature can rise above 600 °C. Flashover with adequate air

intake through openings can give a big fire. The whole room will then become a big burning object. There are three main points to judging the critical conditions (Fan et al. 2014).

- The heat flux received by the combustibles on the interior ground-floor reaching 20 kW/m^2;
- The temperature of the air below the ceiling reaching close to 600°C;
- The burning rate being over 40 g/s. Satisfying one of the above conditions can be considered as a flashover. For different buildings, the critical conditions are different.

This paper chose the temperature of the smoke near the roof being close to 600°C when the flame spread to the top of the temple as the critical condition.

3. Results and Discussion

In order to respond to the objective, the fire growth and spread was analyzed in a historic wooden structure temple. The study was developed in two main stages:(1) Basic fire development in the temple, including fire spread, HRR and temperature, smoke spread, CO_2 & CO concentration; (2) Parameter settings that affect the fire spread, including wood pyrolysis kinetics parameters, reference temperature (RT) and wood density.

3.1 Basic fire development in the temple

The time variation of flashover time in different conditions was shown in Table 5. The fire spread trends during fire growth were aligned, but flashover time of Spruce issued 10~20 sec earlier than that of the other three historical wood (Cases1~ 4). Take the Spruce burning case as an example to analyzing the basic fire development of the early stage in the temple. Details of the fire spread are discussed as following.

3.1.1 The spread of the fire

Figure 6 shows the process of fire spread. Due to buoyancy, flame tended to ascend vertically upwards and spread to the roof at about 300 sec. From 300 sec to 360 sec, we found that fire tilted increasingly towards the fuel bed pushing the flame towards the unburned region of the roof board. At 360 sec, flames ignited purlins, beams, lookouts, rafters, etc, which indicated that a flashover was on the way. The fire ignited the four corners of the temple and was soon filled with flame around 420 sec. The ingress of outdoor air contributed to the burning of wood within the boundaries of the building. In addition, flames gushing out of the windows & doors was common.

3.1.2 The HRR and temperature variation

The time variation of the HRR was showed in Figure 7(a). Before 260 sec, the HRR was at a low level and started to rapidly increase with more and more severe development of the fire at 360 sec. At approximately 480 sec, the HRR reached its maximum value, 750 MW. Figure 7(b) presents the temperature distribution obtained from thermocouples: the temperature was lower as the fire spread slowly in the early stage (before 260 sec), and the indoor temperature rose to above 600°C around 360 sec with a flashover taken place, after which the indoor temperature started to gradually decrease but still above 300°C.

Figure 8 illustrated slice of temperature distribution across two sections at 360 sec. It can be seen from a-a section that temperature near the sloped roof exceeded 600°C. In the same slice, the temperature increased gradually when height was increased and the highest temperature was near the sloped roof. Since there was a lot of fire load on the roof, it produced more heat when it burnt. Hence, it strongly suggested that the radiation heat contribute significantly

towards promoting fire spread on a sloped roof, driven by the upslope wind induced by the fire. As can be seen from b-b section that temperature in the left part of the temple was higher than that of the right part. In other words, the fire in the left part was more serious than that in the right part. That was because there were more movable fire loads in the left part of the temple. Therefore, it'd better to optimize the distribution of indoor movable fire loads to reduce the occurrence of fire or lessen the severity of fire.

From the simulation data and gushing out of flames under visual observation, one can be sure that flashover occurred at around 360 sec. Therefore, the judgment of flashover occurrence based on the temperature of 600°C near the roof was reliable.

3.1.3 The spread of the smoke

The smoke layer can be visualized through three-dimensional plots as shown in Figure 9 (a). From Figure 9(a) we can find that smoke started to accumulate on the sloped roof under the action of buoyancy after the temple caught fire. At 120 sec, smoke spread up to the wall, after hitting the roof, it began to accumulate and spread around. At 240 sec, smoke filled the entire ridge. At about 360 sec, smoke filled the entire temple. Since no mechanical exhaust device in the temple, smoke can spread out through the windows & doors and other gaps in the building. As can be seen in Figure 9(a), the simulation result was able to replicate the smoke spread behaviour. Figure 9(b) illustrates the smoke concentration variation at H=2 m, 3 m, 5 m. The smoke concentration was less than 20%/m before 100 sec due to the fire spread slowly at the beginning of combustion. From 150 sec to 400 sec, the smoke concentration increased rapidly as the fire gradually entered the full development stage. Before 400 sec, the smoke concentration at H=5 m was always higher than that at H=3 m and H=2 m. At around 400 sec,

the concentration of smoke reached 100% with the visibility dropped to zero.

From Figure 9(a) we can find that the upward propagation speed of smoke was faster than that horizontally. Meanwhile, smoke tended to flow upwards driven by buoyancy and accumulated. That phenomenon was often referred to as "the stack effect." The stack effect was the main driving force behind the upward flow of smoke.

Figure 9(c)shows the visibility variation at different heights in the temple. Before 120 sec of the fire, visibility was almost at the same level and was all above 10 m. Between 120 sec and 300 sec, smoke and soot particles continued to spread upwards under the action of buoyancy and the visibility was constantly decreasing. The more smoke accumulated, the poorer the visibility was, and the visibility at H=5 m is lower than that at H=3 m and H=2 m before 400 sec. At around 400 sec, visibility was down to nearly 0 m in the temple.

3.1.4 The variations of CO_2 & CO concentration

Figure 10(a) shows the CO_2 concentration variation. The CO_2 concentration stayed a low level in the early stage of the fire, and gradually increased to 0.04 kg/m^3 from 120 sec to 240 sec. Between 300 sec and 330 sec, the CO_2 concentration appeared a “jumping” due to the unstable combustion process or the short-term weakening of the fire when the fire spread from one position to another. The CO_2 concentration reached about 0.1 kg/m^3 after 460 sec.

Figure 10(b) shows the CO concentration variation. The CO concentration was not increased until 150 sec. Between 360 sec and 380 sec, the CO concentration also appeared a “jumping”. We speculated that the combustion process of indoor combustibles was unstable or the supply of air was relatively insufficient during combustion. After 400 sec, the CO concentration gradually increased and reached about 0.013 kg/m^3 at 800 sec.

3.2 Factors affecting the spread of fire

There are many factors affecting the fire spread. When choosing the option of inputting pyrolysis parameters and the density of combustible material, the influences of pyrolysis parameters of fresh wood and historical wood on fire spread were analyzed. When choosing the option of inputting RT and the density of combustible material, the influences of different RT as well as the density of wood on fire spread were analyzed. Besides, the two options of parameter setting were compared and analyzed. The conclusions are reasonably proved by comparison derived from full-scale tests performed on FDS.

3.2.1 Effect of wood pyrolysis parameters and density

In this paper, a large number of literatures were reviewed, the pyrolysis parameters of some fresh wood were obtained and simulated. In order to control for a single variable, we set the density to 410 kg/m^3. Cases 5 ~ 8 in Table 5 presented fire experimental results of four types of relatively fresh wood. Torch pine was the first to occur a flashover, at 450 sec, which was 90 sec later than that compared with that of Spruce in Case 3. The flashover time of other three fresh wood was even later and no flashover of Masson pine in 800 sec.

Compared the pyrolysis parameters in Cases 1 ~ 8, we can find that pyrolysis parameters (including Pre-reference factor and apparent activation energy) of historical wood were smaller than those of fresh wood. The results demonstrated the smaller the pyrolysis parameters were, the faster fire spread and the sooner flashover occurred.

3.2.2 Effect of RT and density

To study the effect of wood density and RT on fire spread, we chose the other option of

parameter setting to run fire spread process by inputting RT and the density of combustible material. Numerical simulations with the same temple model to predict the fire features, the results were shown in Table 5 in Cases 9 ~ 12. We can see that the setting of RT=150°C and the wood density of 410 kg/m^3 in Case 9 was relatively reasonable and credible as the simulation result was consistent with the results in Case 3. Meanwhile, comparing Cases 9 ~ 12, we can easily find that the lower the RT was, the shorter the time of flashover was.

To further explore the influence of wood density on flashover time, additional different wood density settings were added in Case 13 and Case 14 in Table 5. Compared the results of wood5 (561.8 kg/m^3) and wood6 (640 kg/m^3) with that of wood1(410 kg/m^3), we can find that flashover time of wood1 was 100 sec ~ 310 sec earlier than that of wood5 and wood6 separately. We concluded that the lower the density of wood was, the sooner flashover occurred.

4. Conclusions

In this study, in-situ fire load surveys were carried out in an accredited historical wooden structure temple in use in Beijing. Besides, pyrolysis kinetics parameters and physical parameters of historical raw wood were obtained by wood thermogravimetric experiments and cone calorimeter and electronic balance tests. Numerical simulations were performed to study fire spread characteristics in historic wooden buildings. Finally, by comparing the results of flashover time in different experiment conditions, we discovered the influences of different parameter settings on fire spread. The results show that this method can reflect the varying of scenes of historic wooden buildings indoor fire accurately, and the results can provide references for the fire spread characteristics of historic wooden structure buildings. The conclusions are as following:

(1) There was a large of fire load in the historic wooden structure temple, the fixed fire load density was about 4,383.88 MJ/m^2, the movable fire load density was about 970.21 MJ/m^2, the total fire load density was about 5,354.09 MJ/m^2. The total fire load density of the historic wooden structure temple was about 6.86 times ~ 12.75 times that of the houses and the offices.

(2) Four types of historical wood have little difference in physical properties except density. The highest density of Nanmu was 561.8 kg/m^3, followed by White pine (505.9 kg/m^3) and Red pine (413.7 kg/m^3), and Spruce (386.0 kg/m^3) was the lowest.

The maximum pyrolysis kinetics parameters of Spruce were the largest, Pre-reference factor was 2.12×10^6 1/min and apparent activation energy was 83,020 kJ/kmol. The minimum of the pyrolysis kinetics parameters of White pine were the smallest, Pre-reference factor was 3.08×10^5 1/min and apparent activation energy was 75,120 kJ/kmol. Meanwhile, the pyrolysis kinetics parameters of historical wood were smaller than those of fresh wood, leading to the fire spread faster and flashover occurred more than 90 sec earlier than that of fresh wood.

(3) There was no significant difference in the flashover time of four kinds of historical wood. Spruce occurred a flashover at about 360 sec, White pine and Red pine occurred at about 370 sec, while Nanmu occurred at about 380 sec.

(4) The direction of smoke spread in a historic wooden temple usually follows this path: near the fire source → vertical rising → titled towards the sloped roof → hit the top board → spread horizontal and downward. The characteristic of fire spread is: fire spread is slowly in the early stage, when it spread to the roof of the temple, it will easily occur a flashover and spread in the whole room.

(5) It is reasonable to set RT=150°C with wood density of 410 kg/m^3 in the fire simulation of

wood structure buildings. At the same time, flashover time of that was 100 sec and 310 sec earlier than that with wood density of 561.8 kg/m^3 and 640 kg/m^3 separately.

Fire prevention measures are as follows:

(1) The historic wooden temple has a large of fire loads, which should be properly reduced in order to reduce fire risks. Strengthen control of the fire sources: strictly control the use of candles, fireworks and the incense burners around the temple.

(2) Strengthen fire protection of the roof. To reduce the fire damage, the fire suppression system should be started within 6 minutes after the fire.

(3) In the principle of not affecting the architectural style and the value of cultural relics, fire-retardant technology should be used to treat wood beams and pillars with fire-retardant coatings and flame-retardant liquids. For non-relic fabrics that are not frequently replaced in historic buildings, such as curtains, temporary retardant treatment can be used.

Disclosure Statement

The authors declare no conflicts of interest.

Acknowledgements

This research was funded by Beijing Science and Technology Plan Project--Research and Application Demonstration of Electrical Fire Monitoring and Fire Prevention Technology for Cultural Relics, no. Z171100004417031, China.

References

Altun, Y., M. Doğan, and E. Bayraml. 2016. Flammability and thermal degradation behavior of flame retardant treated wood flour containing intumescent LDPE composites. *European*

Journal of Wood and Wood Products 74(6), 851-856. doi:10.1007/s00107-016-1042-1.

Bartlett, A. I., R. M. Hadden, J. P. Hidalgo, S. Santamaria, F. Wiesner, L. A. Bisby, S. Deeny, and B. Lane. 2017. Auto-extinction of engineered timber: Application to compartment fires with exposed timber surfaces. *Fire Safety Journal* 91:407-13. doi:10.1016/j. fire saf. 2017.03.050.

Bernardini, G., M. Azzolini, M. D'Orazio, and E. Quagliarini. 2016. Intelligent evacuation guidance systems for improving fire safety of Italian-style historical theatres without altering their architectural characteristics. *Journal of Cultural Heritage* 22:1006-18. doi:10.1016/j.culher. 2016.06.008.

Byström, A., X. Cheng, U. Wickström, and M. Veljkovic. 2012. Full-scale experimental and numerical studies on compartment fire under low ambient temperature. *Building and Environment* 51 (C):255-62. doi:10.1016/j.buildenv.2011.11.010.

Bianchi, O., J. D. N. Martins, R. Fiorio, R. V. B. Oliveira, and L. B. Canto. 2011. Changes in activation energy and kinetics mechanism during eva crosslinking. *Polymer Testing* 30(6), 616-624. doi:10.1016/j.polymertesting.2011.05.001.

Chorlton, B., and J. Gales. 2020. Fire performance of heritage and contemporary timber encapsulation materials. *Journal of Building Engineering* 29 (2020) 101181. doi:org/10.1016/j.jobe.2020.101181.

Chorlton, B., and J. Gales. 2019. Fire performance of cultural heritage and contemporary timbers. *Engineering Structures* 201 (2019) 109739. doi:org/10.1016/j.engstruct.2019.109739.

Chen, T.B.Y., A.C.Y. Yuen, C. Wang, G.H. Yeoh, V. Timchenko, S.C.P. Cheung, Q.N. Chan, and W. Yanga. 2018. Predicting the fire spread rate of a sloped pine needle board utilizing

pyrolysis modelling with detailed gas-phase combustion. *International Journal of Heat and Mass Transfer* 125 (2018) 310–322. doi: 10.1016/j.ijheatmasstransfer.2018.04.093.

Chen, C. J., W. D. Hsieh, W. C. Hu, C. M. Lai, and T. H. Lin. 2010. Experimental investigation and numerical simulation of a furnished office fire. *Building and Environment* 45(12):2735-42. doi:10.1016/j.buildenv.2010.06.003.

Chow, C.L., and W.K. Chow. 2010. Heat release rate of accidental fire in a supertall building residential flat. *Building and Environment* 45:1632-1640. doi:10.1016/j.buildenv.2010.01.010.

Cordero, T., F. García, and J. J. Rodríguez. 1989. A kinetics study of holm oak wood pyrolysis from dynamic and isothermal TG experiments. *Therm-ochimica Acta* 149: 225-237. doi:10.1016/0040-6031(89)85284-0.

Dong, Q., F. You, and S.-Q. Hu. 2014. Investigation of Fire Protection Status for Nanjing Representative Historical Buildings and Future Management Measures. *Procedia Engineering* 71: 377-384. doi: 10.1016/j.proeng.2014.04.054.

Durak, S., Y. Erbil, and N. Akıncıtürk. 2011. Sustainability of an Architectural Heritage Site in Turkey: Fire Risk Assessment in Misi village. *International Journal of Architectural Heritag* 5:334-348. doi:10.1080/ 1558305100 3642721.

Emberley, R., C. G. Putynska, A. Bolanos, A. Lucherini, A. Solarte, D. Soriguer, M. G. Gonzalez, K. Humphreys, J. P. Hidalgo, C. Maluk, A. Law, and J. L. Torero. 2017. Description of small and large-scale cross laminated timber fire tests. *Fire Safety Journal* 91:327-35. doi:10.1016/j. firesaf.2017.03.024.

Fan, W.-C., J.-H. Sun, S.-X. Lu, Z.-L. Yang, G.-X. Liao, H.-Y. Yuan, H. Yuan, Bin, Y., T.-Z. Hu, and Z-B. Fang. 2014. *Fire Risk Assessment Methodology.* Beijing, Science Press.

Yan, H.-P., X.-X. Lu, and T.-F. Qin. 1997. Study on Chemical Kinetics of Wood Pyrolysis by Thermogravimetric Analysis. *Chinese Journal of Wood Industry* 11(2): 14-18. doi:CNKI:SUN:MCGY.0.1997-02-003.

Gašparovič, L., J. Labovský, J. Markoš, and L'. Jelemenský. 2012. Calculation of kinetics parameters of the thermal decomposition of wood by distributed activation energy model (DAEM). *Chemical & Biochemical Engineering Quarterly* 26(1), 102-114. doi:10.1007/978-94-011-7352-0_21.

GB 2677.1-1993. 2004. Fibrous raw material of sampling for analysis.

Huang, D.-M., C.-M. Xu, L.-M. Li, Y. Li, H.-P. Zhang, H. Yang, and L. Shi. 2011. Recent Progresses in Research of Fire Protection on Historic Buildings. J*ournal of Applied Fire Science* 19(1):63-81. doi:10.2190/AF.19.1.d.

Hao, C., and G. V. Hadjisophocleous. 2011. Dynamic modeling of fire spread in building. *Fire Safety Journal* 46:211-224. doi:10.1016/j.firesaf.2011.02.003.

Hadjisophocleous, G., and Q. Jia. 2009. Comparison of FDS Prediction of Smoke Movement in a 10-Storey Building with Experimental Data. Carleton University, Ottawa, ON, Canada. *Journal of Fire Technology* 45:163-177. doi:10.1007/s10694-008-0075-3.

Ibrahim, M.N., K. Abdul-Hamid, M.S. Ibrahim, A. Mohd-Din, R.M. Yunus, and M.R. Yahya. 2011. The development of fire risk assessment method for heritage building. *Procedia Engineering* 20:317-24. doi:10.1016/j.proeng.2011.11.172.

Lowden, L.A., and T. R. Hull. 2013. Flammability behaviour of wood and a review of the methods for its reduction. *Fire Sci Rev* 2(4):1-19. doi:10.1186/2193-0414-2-4.

Li, H.-Q., Y. Yu, and X. Yu. 2012. On Fire Protection Problems and Its Countermeasures about

Chinese Ancient Architecture. *Applied Mechanics and Materials* 204(208): 3365-3368. doi:10.4028/www.scientific.net/AMM.204-208.3365.

Lu, W.-L. and J.-X. Cheng. 2012. Numerical Simulation Analysis of Fire in Ancient Building burning Temple. *Fire Science and Technology* 04:290-293. doi:10.3969/j.issn.1009-0029.2011.04.006.

Meng, Q.-X., G.-Q. Zhu, M.-M. Yu, and R.-L. Pan. 2018. The effect of thickness on plywood vertical fire spread. *Procedia Engineering* 211:555-564. doi:10.1016/j.proeng.2017.12.048.

Mohomane, S.M., T.E. Motaung, and N. Revaprasadu. 2017. Thermal Degradation Kinetics of Sugarcane Bagasse and Soft Wood Cellulose. *Materials* 10(11): p. 1246. doi:10.3390/ma10111246.

Matsushima, D., and T. Takaya. 2017. Fire spreading simulation of a group of wooden houses. Reports of the Information and Computer Science Center (45):16-42. in Japanese.

Matheus, P., A. J. Zattera, and R. M. C. Santana. 2012. Thermal decomposition of wood: kinetics and degradation mechanisms. *Bioresour Technol* 126:7-12. doi:10.1016/j.biortech.2012.08.133.

McGrattan, K. B., S. Hostikka, J. E. Floyd, H. R. Baum, and R.G. Rehm. 2007. *Fire dynamics simulator (version 5)*, technical reference guide. Gaithersburg, Maryland: National Institute of Standards and Technology.

Neto, J.T., T. M. Ferreira. 2020. Assessing and mitigating vulnerability and fire risk in historic centres: A cost-benefit analysis. *Journal of Cultural Heritage* 45 (2020) 279–290. doi:org/10.1016/j.culher.2020.04.003.

Östman, B., D. Brandon, and H. Frantzich. 2017. Fire safety engineering in timber buildings.

Fire Safety Journal 91:11-20. doi:10.1016/j.firesaf.2017.05.002.

Östman, B., and L. Tsantaridis. 2016. Durability of the reaction to fire performance for fire retardant treated (FRT) wood products in exterior applications-A ten years report. Paper presented at the 2nd International Seminar for Fire Safety of Facades, Lund (Sweden), *MATEC Web of Conferences* 46:05005. doi:10.1051/matecconf/ 20164605005.

Poletto, M., A.J., Zattera, and R.M.C. Santana. 2012. Thermal decomposition of wood: kinetics and degradation mechanisms. *Bioresour Technol* 126:7-12. doi:10.1016/j.biortech.2012.08.133.

Richter, F., and G. Rein. 2020. A multiscale model of wood pyrolysis in fire to study the roles of chemistry and heat transfer at the mesoscale. *Combustion and Flam*e 216. 316–325. doi:10.1016/j.combustflame.2020.02.029.

Regueira, R., and M. Guaita. 2018. Numerical simulation of the fire behaviour of timber dovetail connections. *Fire Safety Journal* 96:1-12. doi:10.1016/j.firesaf.2017.12.005.

Watts, J. M., and R.E. Solomon. 2002. Fire safety code for historic structures. *Fire Technology* 38(4). doi: 10.1023/A:1020110214065.

Schmid, J., M. Klippel, A. Just, and A. Frangi. 2014. Review and analysis of fire resistance tests of timber members in bending, tension and compression with respect to the Reduced Cross-Section Method. *Fire Safety Journal* 68:81-99. doi:10.1016/j.firesaf.2014.05.006.

Sanchez-Silva, L., D. López-González, J. Villaseñor, P. Sánchez, and J. L. Valverde. 2012. Thermogravimetric-mass spectrometric analysis of lignocellulosic and marine biomass pyrolysis. *Bioresource Technology* 109(none), 163-172. doi: 10.1016/j.biortech.2012.01.001

Sun R.Y., M. A. Jenkins, S. K. Krueger, W. Mell, and J. J. Charney. 2011. An evaluation of fire-plume properties simulated with the Fire Dynamics Simulator (FDS) and the Clark

coupled wildfire model. *Canadian Journal of Forest Research* 36(11): 2894-2908. doi:10.1139/x06-138.

Tung, S.F., H.-C. Su, C.-T. Tzeng, and C.-M. Lai. 2018. Experimental and Numerical Investigation of a Room Fire in a Wooden-Frame Historical Building. *International Journal of Architectural Heritage*. doi: 10.1080/15583058.2018.1510999.

Tian, D.-H., X.-S. Wu, Z.-G. Song, and H.-Y. Wang. 2016. Reverse analysis for fire pyrolysis parameters of timber buildings based on response surface method. *Procedia Engineering* 135:19-24. doi:10.1016/j.proeng.2016.01.073.

The State Administration of Cultural Heritage and the Ministry of Public Security issued the Ten Provisions on Fire Safety Management of Cultural Relics Buildings, 2015. *Fire Industry* (01):46.

Tapasvi, D., R. Khalil, G. Várhegyi, K.-Q. Tran, M. Grønli, and Ø. Skreiberg. 2013. Thermal Decomposition Kinetics of Woods with an Emphasis on Torrefaction. *Energy Fuels* 27:6134-6145. doi:10.1021/ef4016075.

Wang H., N. Jia, and Y. Xin. 2017.Thermogravimetric analysis experiment and kinetics analysis of wood. *Fire Science and Technology* 36(09), 1209-1212. doi:10.3969/j.issn.1009-0029.2017.09.009.

Weinschenk, C.G., J. K. Overholt, and D. Madrzykowski. 2016. Simulation of an Attic Fire in a Wood Frame Residential Structure, Chicago, IL. *Fire Technology* 52(6):1629-1658. doi:10.1007/s10694-015-0533-7.

Wen, L.-H., S.-R. Wang, H.-Y. Shi, M.-X. Fang, Z.-Y. Luo, and K.-F. Chen. 2004. Study on pyrolysis characteristics and kinetics of wood. *Journal of Fire Science and Technology* 23(1):

2-5. doi:10.3969/j.issn.1009-0029.2004.01.002.

Zhou, B., H. Yoshioka, T. Noguchi, X. Wang, and C.C. Lam. 2018. Experimental Study on Fire Performance of Weathered Cedar. International *Journal of Architectural Heritage.* doi:10.1080/15583058.2018.1501115.

Zheng, Y.A.N., and B. Liu. 2013. Chinese Historic Buildings Fire Safety and Countermeasure. *Procedia Engineering* 52:23-26. doi:10.1016/j.proeng.2013.02.099.

Zhou, B., X.-M. Zhou, and M.-Y. Chao. 2012. Fire protection of historic buildings: A case study of Group-living Yard in Tianjin. *Journal of Cultural Heritage* 13(4):389-96. doi:10.1016/j.culher.2011.12.007.

Zhu, S., R. Huo, L.-H. Hu, and D. Yang. 2008. Influence of meshing and calculation of regional extension on FDS simulation results. *Journal of Safety and Environment* 8(4):141-145. doi:10.3969/j.issn.1009-6094.2008.04.033.

Table list:

Table 1: Fixed fire loads of the temple hall

Combustion	The hall area 982.36 m^2				Density	Heat of combustion	Total heat of combustion
	L (m)	W (m)	H (m)	Numbers	kg/m^3	MJ/kg	MJ
Area size	46.69	21.04					
Wooden pillars	0.76		6.63	16	410.0	17.95	353,980
	0.76		10.35	16	410.0	17.95	552,593
Purline	0.48		46.69	13	410.0	17.95	807,919
Mortice joints	0.5	0.36	46.69	1	410.0	17.95	61,850.7
	0.39	0.37	46.69	2	410.0	17.95	991,67.3
	0.56	0.38	46.69	4	410.0	17.95	192,623
Beam	0.6	0.37	3.3	8	410.0	17.95	43,132.6
	0.69	0.37	6.6	8	410.0	17.95	99,204.9
	0.89	0.5	10.04	8	410.0	17.95	263,046
	0.59	0.58	16.74	8	410.0	17.95	337,267
Rafter	0.15		21.04	156	410.0	17.95	425,646
Roof board	46.69	21.04	0.1	1	410.0	17.95	722,966
Wooden wall (incl. windows & doors)	42.21	0.12	6.63	1	410.0	17.95	247,149
Total heat of combustion (MJ)							4,107,377
Average heat of combustion (MJ/m^2)							4,383.88

Table 2: Movable fire loads of the temple hall

Combustion	**The hall area 982.36 m²**				**Density**	**Heat of combustion**	**Total heat of combustion**
	L (m)	W (m)	H (m)	Numbers	kg/m³	MJ/kg	MJ
Area size	46.69	21.04					
Display desk	1.1	1.1	0.8	1	410.0	17.95	7,124
	19.2（above the fire）	1.2	0.8	1	410.0	17.95	135,650
	6.0	1.2	0.8	2	410.0	17.95	84,781
	5.5	1.2	0.8	2	410.0.	17.95	77,717
	5.0	1.2	0.8	3	410.0	17.95	70,651
	4.0	1.2	0.8	3	410.0	17.95	84,781
Wood building model	4.8	4.4	1.8	1	410.0	17.95	279,779
Wood shelf	3.6	1.4	3.5	1	410.0	17.95	129,822
Wood sculpture	2.5	2.5	1.8	1	410.0	17.95	82,794
Total heat of combustion (MJ)							953,099
Average heat of combustion (MJ/m²)							970.21

Table 3: Results of thermogravimetric experiment

Wood type	Starting Point(℃)	Peak (℃)	Residual Mass	Activation energy （kJ/mol）	Pre-reference factor （1/min）
White pine	285.2℃	319.3℃	1.38%	75.12	3.08 x10^5
Red pine	290.7℃	317.4℃	1.59%	75.79	3.40 x10^5
Spruce	263.2℃	308.3℃	1.76%	83.02	2.12 x10^6
Nanmu	294.2℃	306.3℃	1.74%	78.45	6.42 x10^5

Table 4: Results of Cone Calorimeter experiment and electronic balance tests

Wood type	**Moisture content (%)**	**Density (kg/m^3)**	**Heat of combustion (MJ/kg)**
White pine	5.44	505.9	23.9
Red pine	4.65	413.7	19.2
Spruce	5.79	386.0	18.6
Nanmu	5.33	561.8	13.6
Variance	0.170	4975.51	13.31

Table 5: Effects of wood pyrolysis kinetics parameters on flashover (four types of historical wood, fresh wood and RT=150 with different wood density) (Yan, H.-P., X.-X. Lu, and T.-F. Qin. 1997)

Condition	Wood type	Ref. Temp (℃)	Density (kg/m^3)	Pre-reference factor（1/min）	Activation energy （kJ/kmol）	Results
Case1	White pine	——	505.9	3.08×10^5	75,120	Flashover at about 370 sec
Case2	Red pine	——	413.7	3.40×10^5	75,790	Flashover at about 370 sec
Case3	Spruce	——	386.0	2.12×10^6	83,020	Flashover at about 360 sec
Case4	Nanmu	——	561.8	6.42×10^5	78,450	Flashover at about 380 sec
Case5	Torch pine	——	410.0	1.18×10^8	85,540	Flashover at about 450 sec
Case6	Lankao Paulownia	——	410.0	1.07×10^8	91,230	Flashover at about 750 sec
Case7	Zhonglin No.1 Yang	——	410.0	3.62×10^8	98,340	Fire spread to the top beam at about 780 sec
Case8	Masson pine	——	410.0	2.05×10^8	98,580	No flashover occurred
Case9	Wood1	150	410.0	——	——	Flashover at about 360 sec
Case10	Wood2	125	410.0	——	——	Flashover at about 220 sec
Case11	Wood3	200	410.0	——	——	Fire spread to the top beam at about 750 sec
Case12	Wood4	250	410.0	——	——	No flashover occurred
Case13	Wood5	150	561.8	——	——	Flashover at about 460 sec
Case14	Wood6	150	640.0	——	——	Flashover at about 670 sec

Figure list:

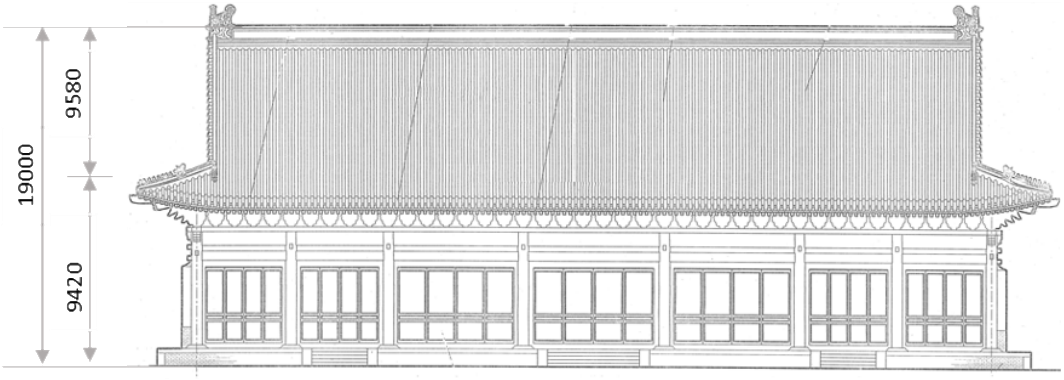

a) Elevation

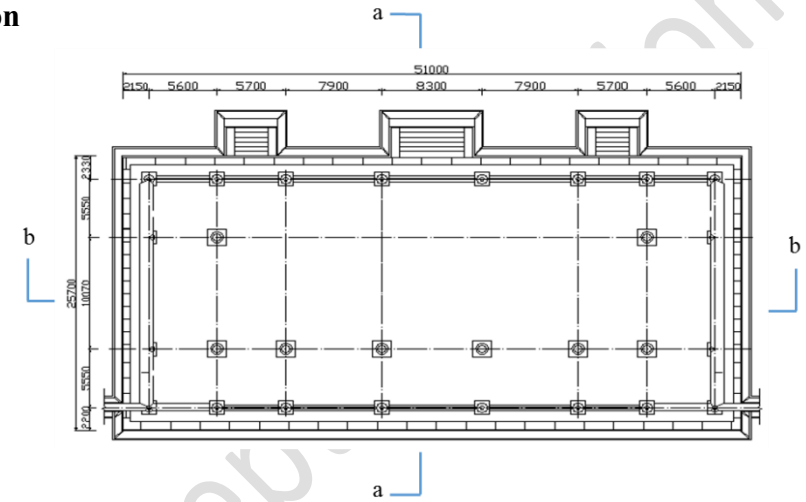

b) Plan (a-a & b-b are the positions of two sections)

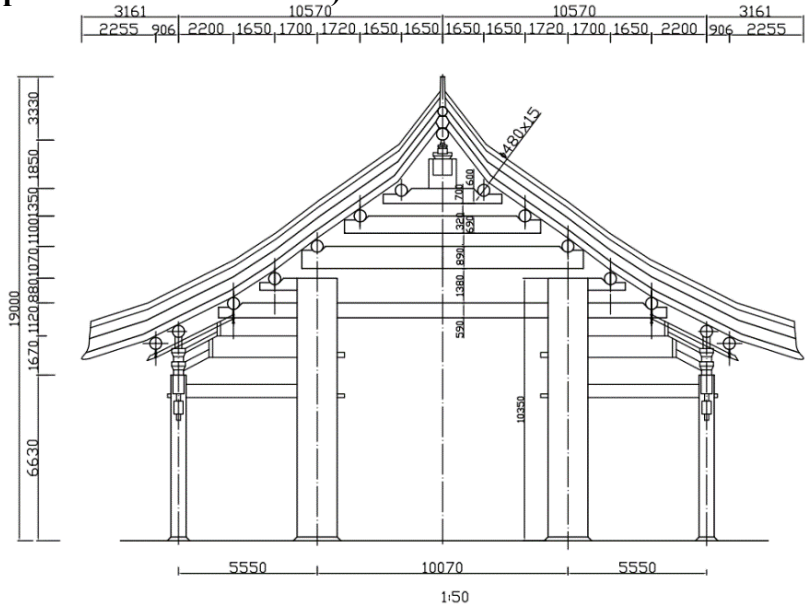

c) Section (a-a)

Figure 1: Elevation, plan and section of the temple hall studied.

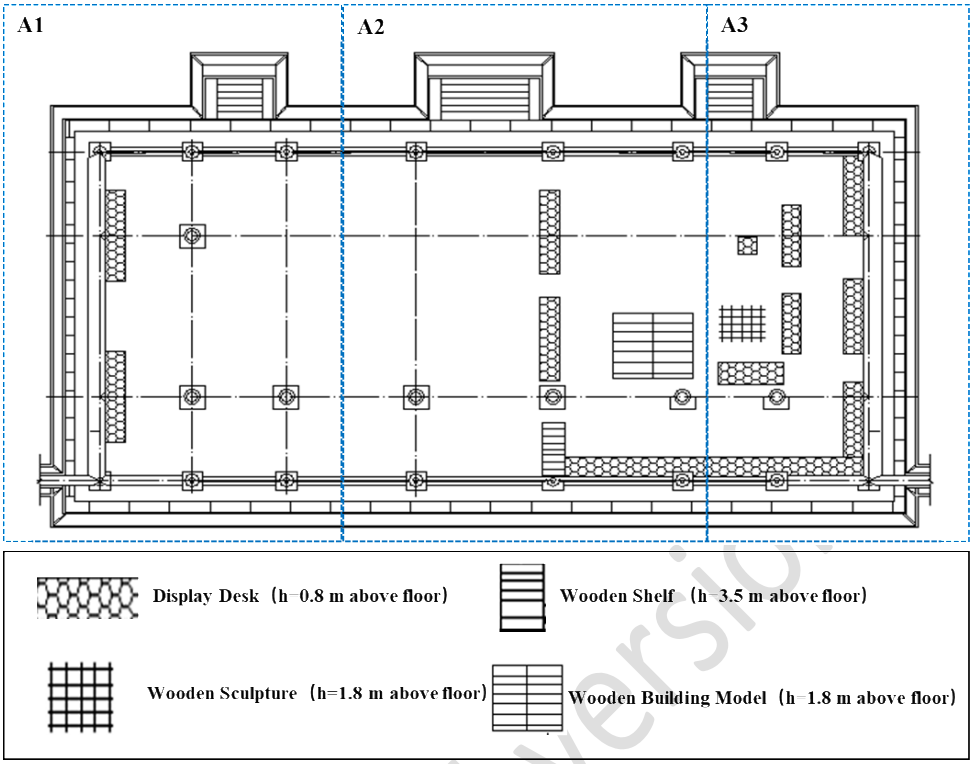

Figure 2. Layouts of indoor furniture in the temple hall (A1, A2 and A3 are three areas).

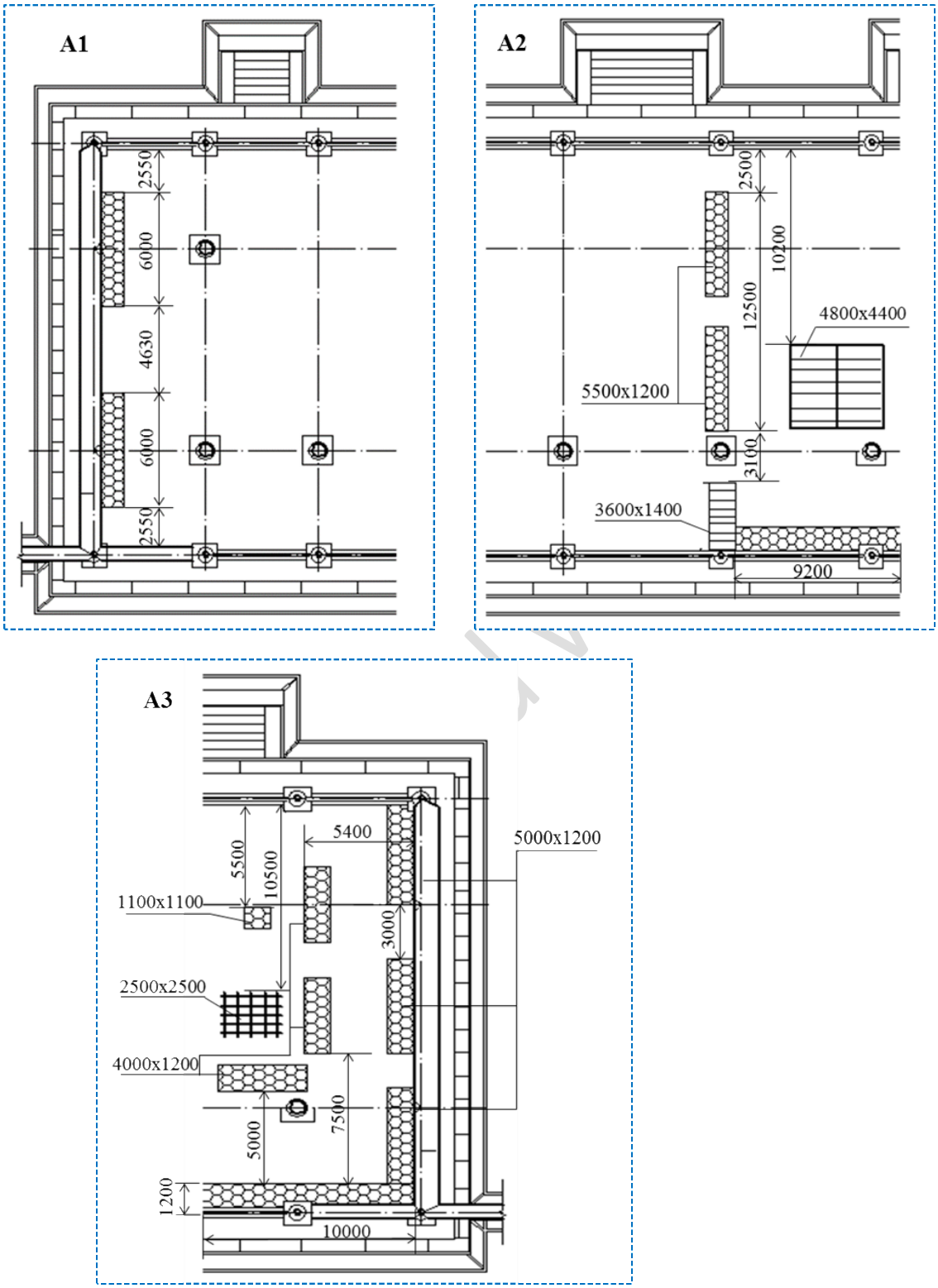

Figure 3. Positions and dimensions of furniture in the hall (A1, A2 and A3 defined in the Figure 2.)

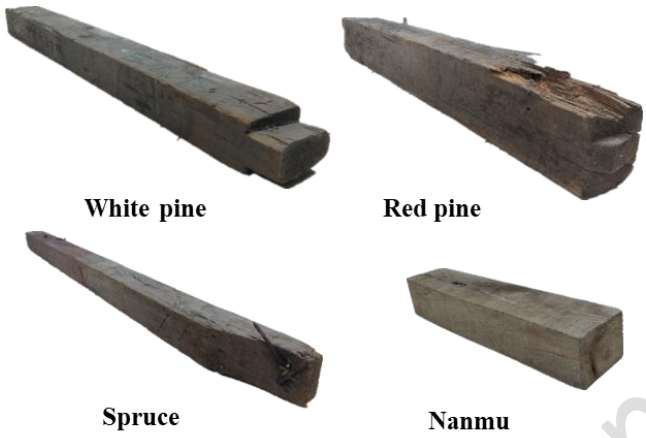

Figure 4. Wood Samples collected from the historic wooden buildings

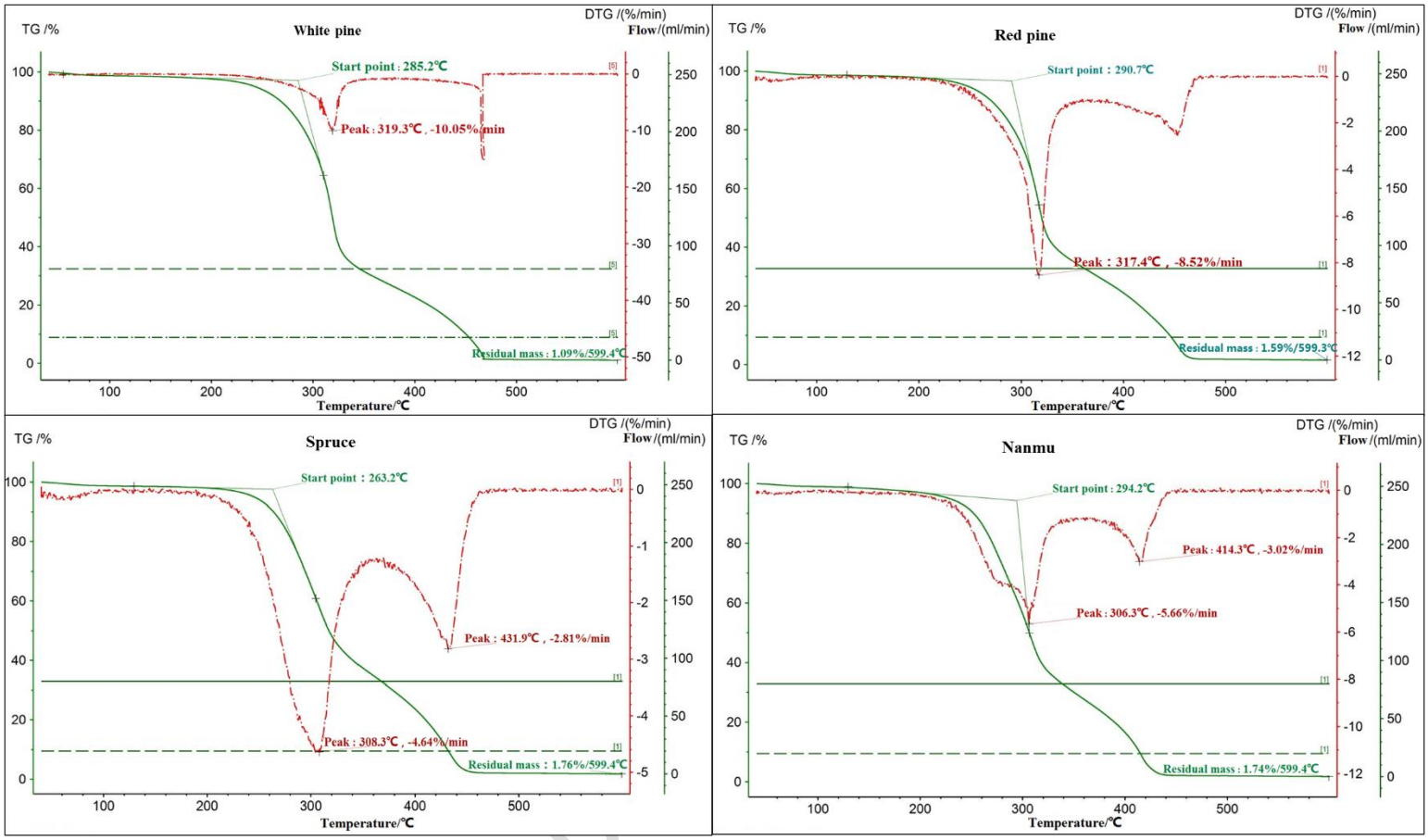

Figure 5. Measured woods pyrolysis process using the Thermogravimetric Analyzer.

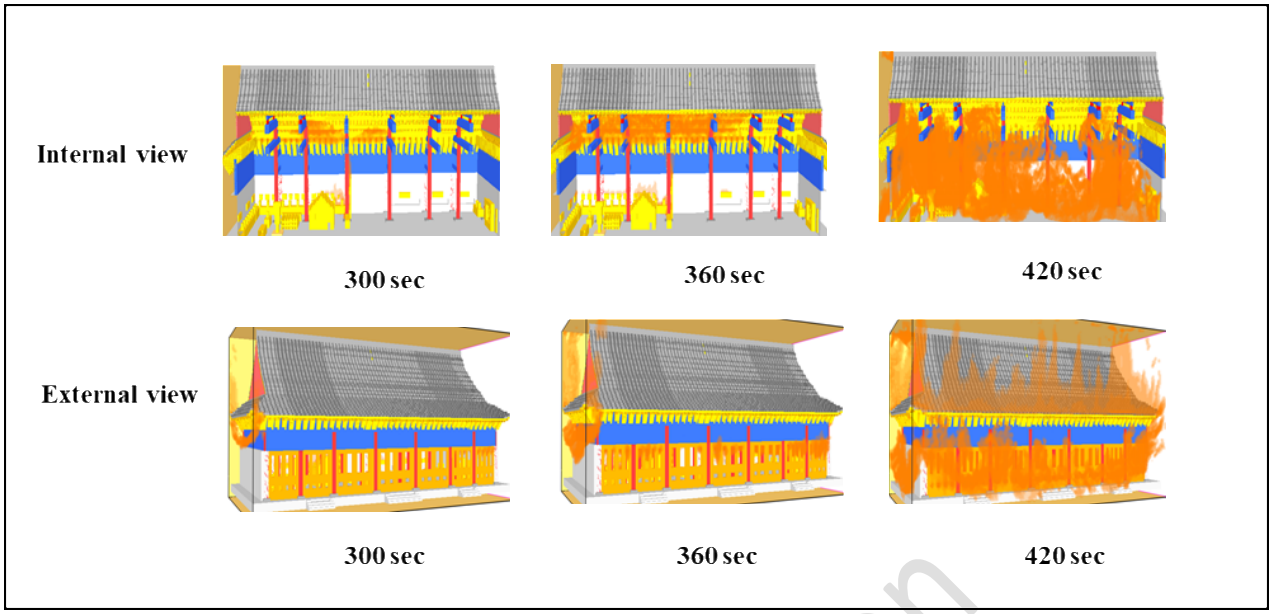

Figure 6. Rendering view of fire spread with the increasing time in the hall (internal and external).

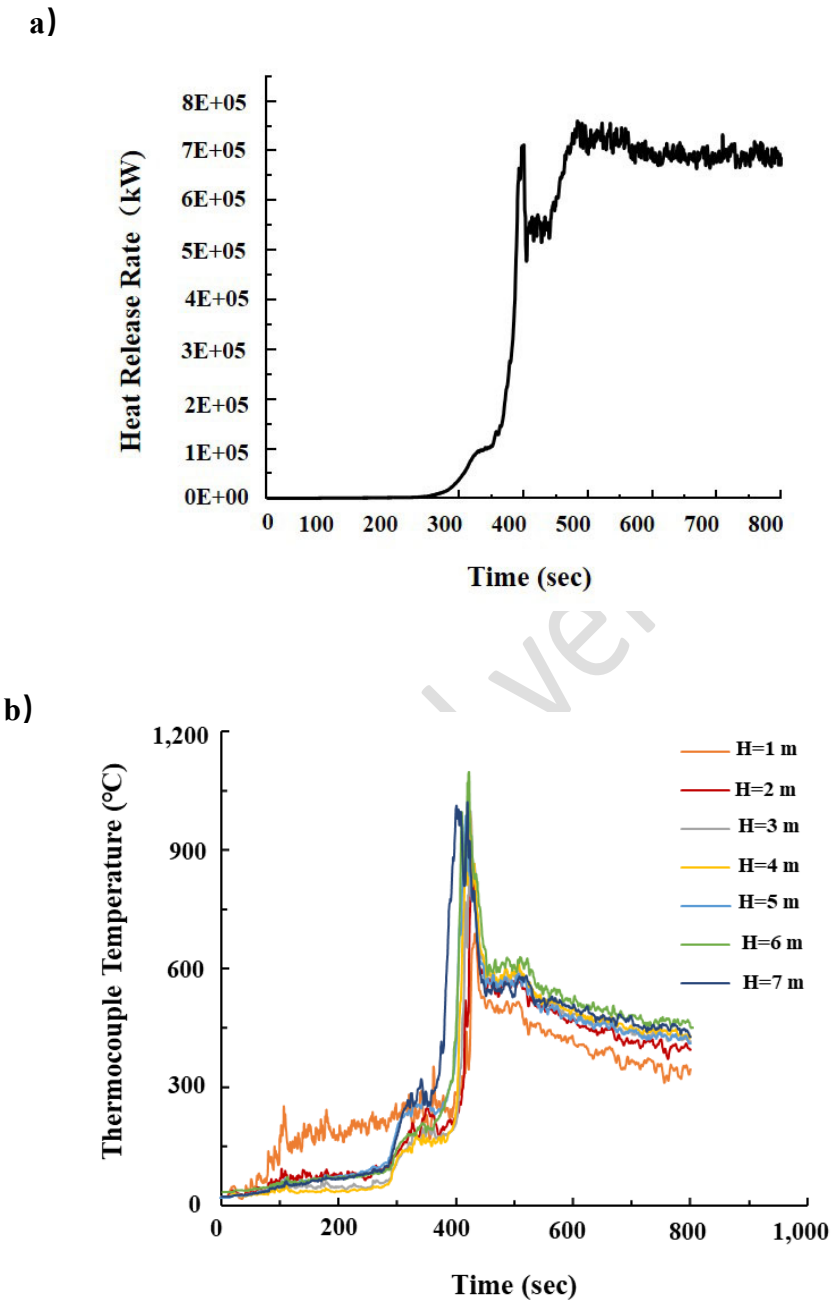

Figure 7. Simulated heat release rate with various times (a); Thermocouple temperature variations with different heights and times (b).

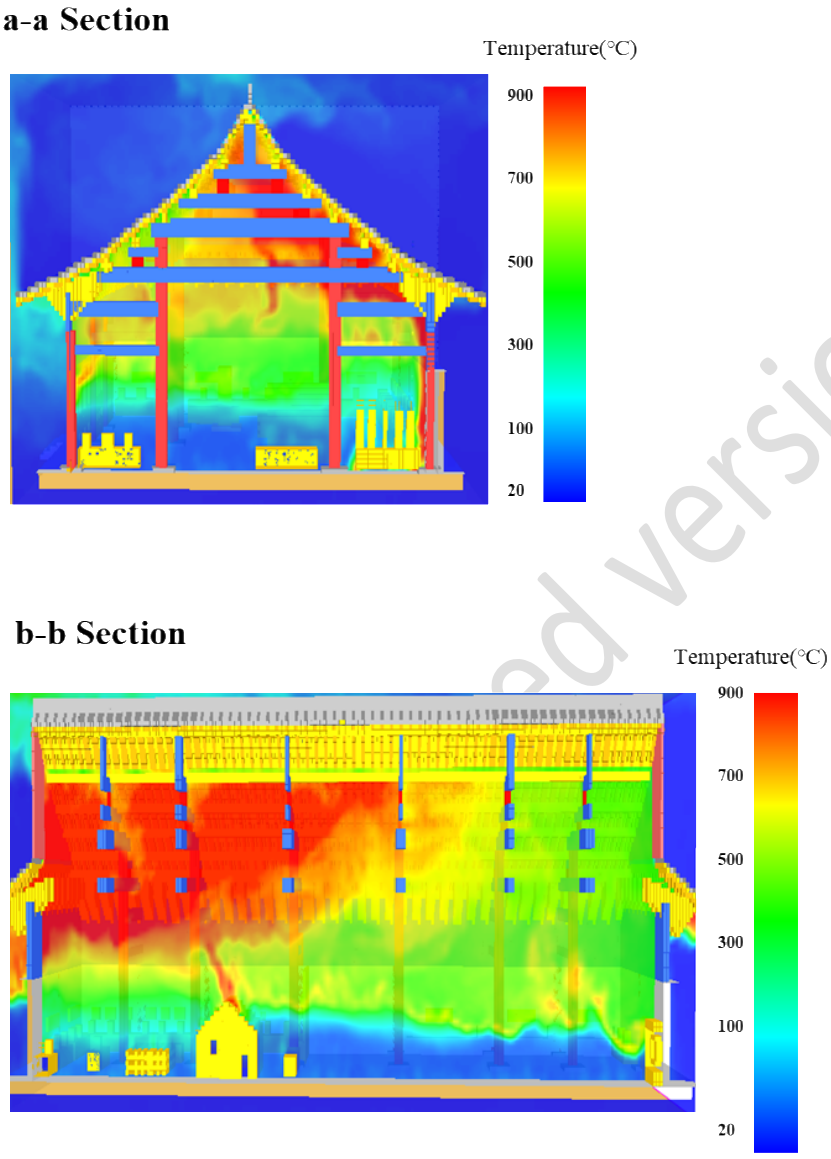

Figure 8. Simulated temperature distributions across two sections (at 360 sec).

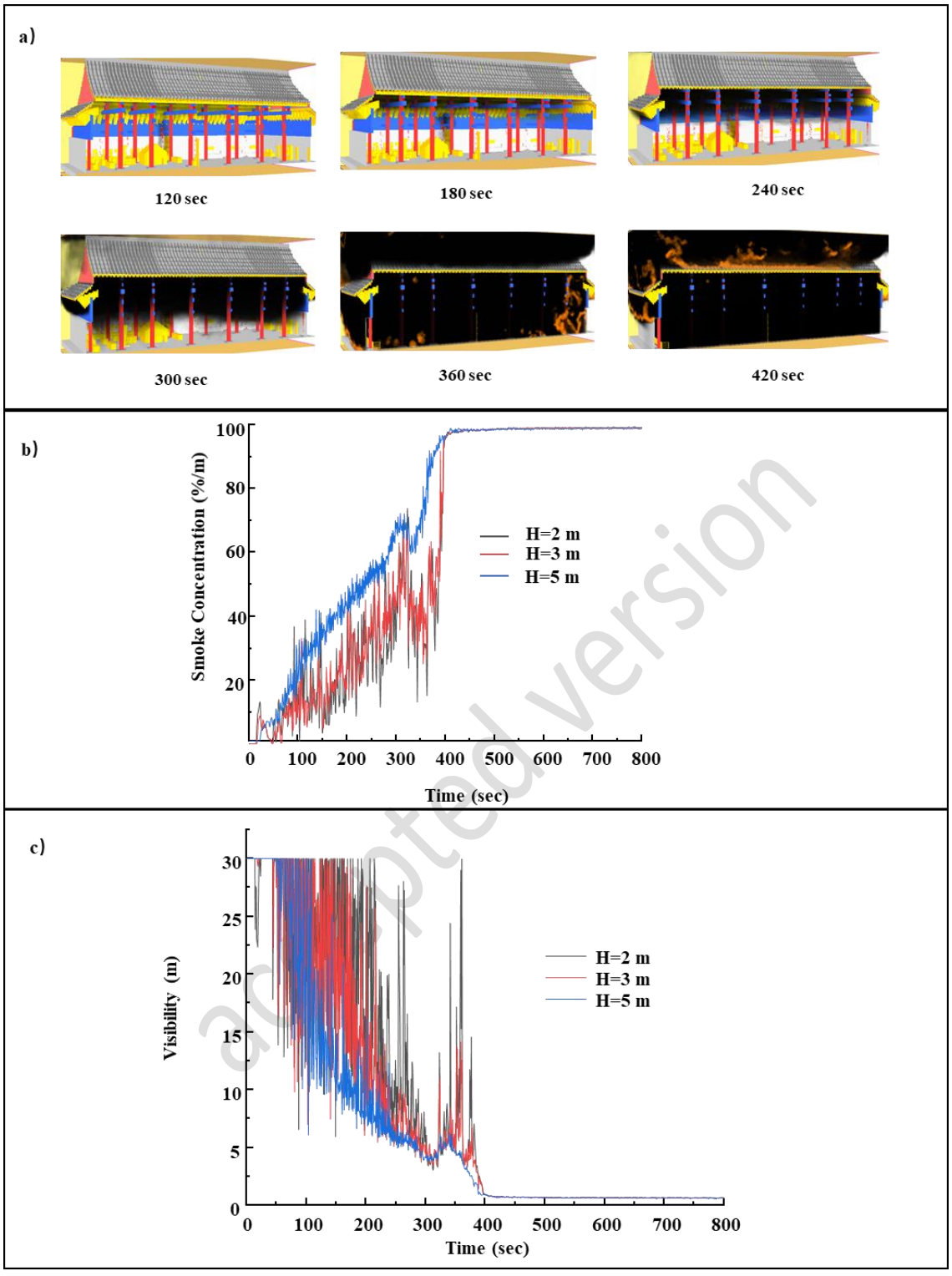

Figure 9. Rendering of smoke spread in the hall with the increasing time (a); Variations of smoke concentration at various heights above the floor (b); Variations of visibility in time at three heights above the floor: 2 m, 3 m and 5 m (c).

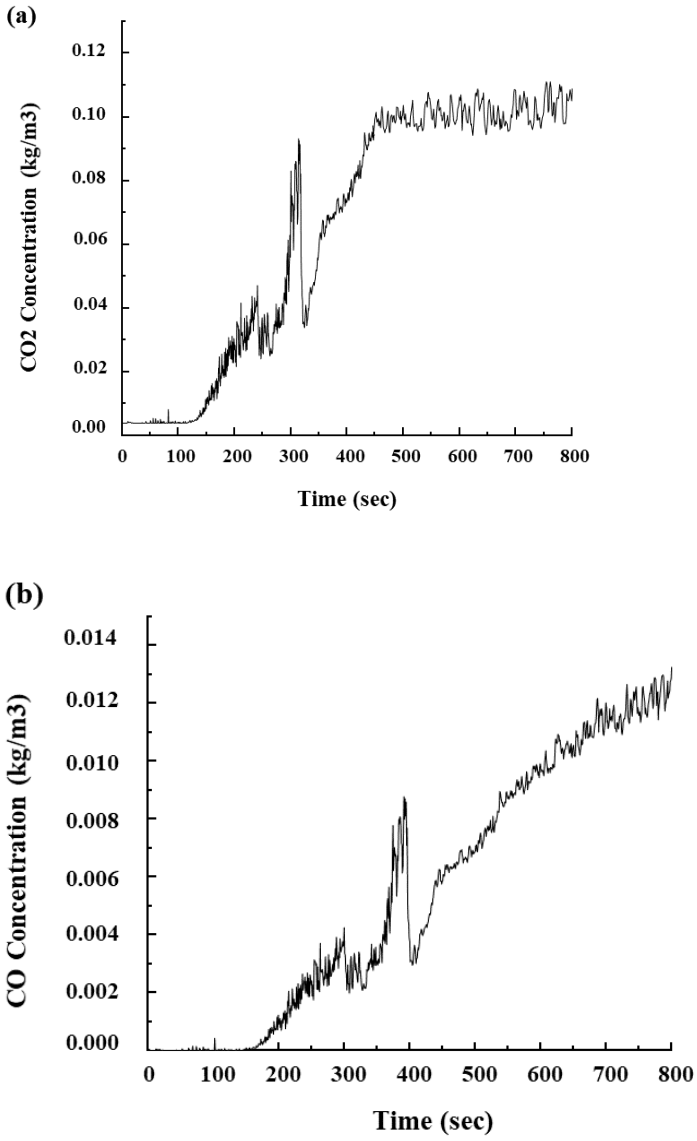

Figure 10. Variations of CO_2 & CO concentration in time.